New Strategies for European Remote Sensing, Oluić (ed.)

Using ASTER and SRTM DEMs for studying geomorphology and glaciation in high mountain areas

Tobias Bolch
Department of Geography, Humboldt University Berlin, Germany

Ulrich Kamp
Department of Geography and Environmental Science Program, DePaul University, Chicago, IL, USA

Jeffrey Olsenholler
Department of Geography and Geology, University of Nebraska - Omaha, Omaha, NE, USA

Keywords: Digital Elevation Model (DEM), ASTER, SRTM, geomorphology, glaciation, Andes, Hindu Kush, Tien Shan

ABSTRACT: For selected peaks in high mountains of diverse climatic regions (Andes, Hindu Kush, Tien Shan) digital elevation models (DEMs) have been generated from Advanced Spaceborne Thermal Emission and Reflection Radiometer (ASTER) data using PCI Geomatica 8.1/8.2 software. Artifacts in the ASTER DEM were eliminated using data from the Space Shuttle Radar Topography Mapping mission (SRTM). For two of the four case studies, accuracy was evaluated by comparison the ASTER/SRTM DEM with DEMs derived from contour maps. Whereas the SRTM DEM shows correct elevations in all altitudes, elevations in the ASTER DEM are slightly to low in higher altitudes and south-exposed aspects. Geomorphic analyses were undertaken using the software ArcInfo, ArcView and SAGA. Cluster analyses including tangetial, vertical curvature and slope combined with spectral information helped identifying debris-covered glaciers and geomorphologic forms and processes. Results show that ASTER/SRTM DEMs are useful for an interpretation of the macro- and mesorelief. The DEM scale sets limits for the level in analysis detail. Whereas SRTM DEMs offer more precise elevations, ASTER DEMs offer more geomorphologic details.

1 INTRODUCTION

A DEM offers the most common method for extracting topographic information and enables the modeling of surface processes. DEMs play an important tool for the analysis of glaciers and glaciated terrains (Bishop et al. 2001, Duncan et al. 1998, Etzelmüller & Sollid 1997, Kaeaeb et al. 2003, Paul et al. 2004, Sidjak & Wheate 1999). To accomplish this, the DEM must represent the terrain as accurately as possible. DEMs can be generated from contour lines, with radar-interferometry data derived, for instance, from Space Shuttle Radar Topography Mapping mission (SRTM), or from stereo satellite data derived from electro-optical scanners such as the Advanced Spaceborne Thermal Emission and Reflection Radiometer (ASTER). This paper presents DEMs derived from SRTM and ASTER data from several high mountain ranges: Andes, Hindu Kush, and Tien Shan.

2 BACKGROUND

2.1 *ASTER and SRTM*

ASTER is a high spatial resolution, multispectral imaging system flying aboard TERRA, a satellite launched in December 1999 as part of NASA's Earth Observing System (EOS). An ASTER scene covering 61.5-km x 63-km contains data from 14 spectral bands. ASTER is comprised of three separate instrument subsystems representing different ground resolutions: three bands in the visible and near infrared spectral range (VNIR, 0.5-1.0 µm) with 15 m spatial resolution, six bands in the shortwave infrared spectral range (SWIR, 1.0-2.5 µm) with 30-m resolution, and five bands in the thermal infrared spectral range (TIR, 8-12 µm) with 90-m resolution. In the VNIR one nadir-looking (3N, 0.76-0.86 µm) and one backward-looking (3B, 27.7° off-nadir) telescope provide black-and-white stereo images, which generate an along-track stereo image pair. During the SRTM mission in February 2000 approx. 80% of the earth surface was measured with methods of radar-interferrometry. Recently, the SRTM DEMs with a resolution of 3" (approx. 90 m) and 1" (approx. 30 m) are available. The 90-m resolution is available free of charge.

2.2 *ASTER DEM generation*

ASTER scenes are distributed in HDF-EOS format, which can be imported by OrthoEngine as part of the PCI Geomatica 8.1/8.2 package. For DEM extraction only the VNIR nadir and backward images (3N and 3B) are used. An automated image-matching procedure is used to generate the DEM through a comparison of the respective gray values of these images. When generated correctly, ASTER DEMs are of sufficient accuracy for many applications, although they are often slightly to low (Bolch & Kamp 2003, Kamp et al. 2003, 2004, Eckert & Kellenberger 2002). Clouds are a major problem in ASTER DEM generation. Elimination of artifacts derived from clouds can be achieved by fitting SRTM data into the "holes". Both data sets have to be georectified, and blending and smoothing procedures will guarantee a seamless transition.

2.3 *Geomorphometric analyses*

Geomorphometric parameters such as elevation, aspect, slope angle, vertical curvature and tangential curvature are useful to identify and describe geomorphological forms and processes, and are extracted using standard software tools. The slope angle helps in identifying geomorphic forms: for example, rectilinear slopes (German: 'Glatthaenge') have a slope angle of 25-35º by definition. Vertical and tangential curvatures are of special interest for morphological and hydrological problems. Geomorphometric analysis helps in explaining meso-scale relief: for instance, a rockglacier front has convex profile and tangential curvatures. Combining the geomorphometric parameters with statistical analyses a classification of surface conditions is possible. The classification can lead into identifying geomorphologic forms (also: glaciers and morrains). As fieldwork in remote high mountain areas is very difficult and time-intensive and the availability of aerial photos is often limited or very expensive, the geomorphometric analysis helps in geomorphological mapping of larger and/or remote areas.

3 MAPPING OF GLACIERS

Several methods of identifying ice from glaciers by means of multispectral remote sensing data are described; especially for Landsat scenes band 4 & 5 (Paul et al. 2002, Sidjak & Wheate 1999). However, debis-covered glaciers are much more difficult to identify, because the spectral signal is similar to the surrounding debris. A new approach to record such glaciers is to include DEM data. This method may also help to map the glaciers, when parts of them are covered by clouds in the remote sensing scene. Bishop et al. (2001) suggested to identify landscape features in a hierarchical approach, where in the last step so called "Terrain Land Form Objects", such as glaciers could be

extracted. Paul et al. (2004) included the slope information to identify debris-covered tongues in the Swiss Alps.

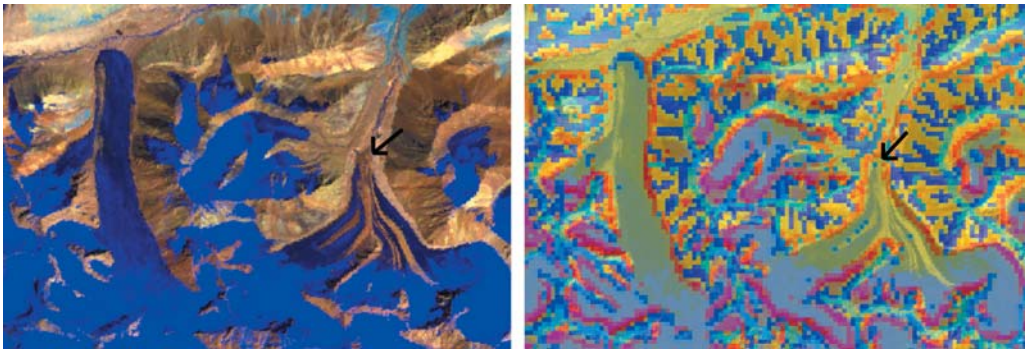

Figure 1. Debis-covered glacier in the Tien Shan. Left: Shown in a Landsat ETM-Scene, bands 7-5-4. Right: Shown with the results of the cluster analysis, including the vertical and tangential curvature as well as the slope derrived from the SRTM DEM with 90 m grid resolution. The arrow shows the end of the glacier.

However, for several glaciers in the semi-arid Tien Shan their method resulted in misinterpretations, e.g. when rock glaciers occur in front of the debris covered glaciers. Therefore we included the vertical and tangential curvature as additional information to the slope. Combining these morphometric parameters in a cluster analysis with eight clusters helped to identify the extend of the glaciers (fig. 1). Including the curvature information yielded especially into better results where only the SRTM data was available, due to cloud cover of the ASTER-Scenes.

4 CASE STUDIES

Studies were carried out in several high mountain ranges of diverse nature (climate, atmospheric conditions, relief): Cerro Sillajhuay (Andes, Chile/Bolivia), Cordillera de Merida (Andes, Venezuela), Tirich Mir (Hindu Kush, Pakistan), and Northern Tien Shan (Kasakhstan/Kyrgyzstan) (Fig. 2).

4.1 *Cerro Sillajhuay, Andes, Chile/Bolivia*

Cerro Sillajhuay (5982 m asl., 19˚45’ S, 68˚42’ W) is located in the Andes at the border between Chile and Bolivia (Fig. 2). It lies in the northern part of the Atacama, which is one of the driest regions on earth. Precipitation in 4500 m asl. is assumed to be only ~200 mm (Bolch & Schröder, 2001). The strato-volcano rises ~2000 m above the surrounding plain. Field work was undertaken in late summer 1998.

The DEM was generated from a cloud-free ASTER level 1A scene from May 2001 (Bolch & Kamp 2003; Kamp et al. 2003, 2004). 12 TPs and 11 GCPs were collected between the stereo-pair. The total $RMSE_{x,y}$ was <17.5 m. The 30-m DEM was generated with the highest possible level of detail and re-sampled to 15-m resolution. The final DEM was compared with a DEM derived from contour lines from a topographical map of 50-m equidistance. Results from geomorphic analysis show that in the ASTER DEM elevations are 89 m to low on average; the peak is 200 m too low. Nevertheless, the ASTER DEM is more accurate when identifying geomorphological features such as rockglaciers, cliff faces, and steep slopes.

Figure 2: Location of study areas.

Both the ASTER DEM and the DEM derived from contour lines were compared with the SRTM DEM of 90-m resolution. There is a very good match between the contour lines extracted from the SRTM DEM and those of the topographic maps. A study for the nearby Salar de Atacama (~22°30' S, ~68° W) showed similar results (Hahn 2003). The extent of Late Quaternary glaciation could be reconstructed and visualized with the software Genesis II using the ASTER DEM, aerial photos, and field data (Fig. 3).

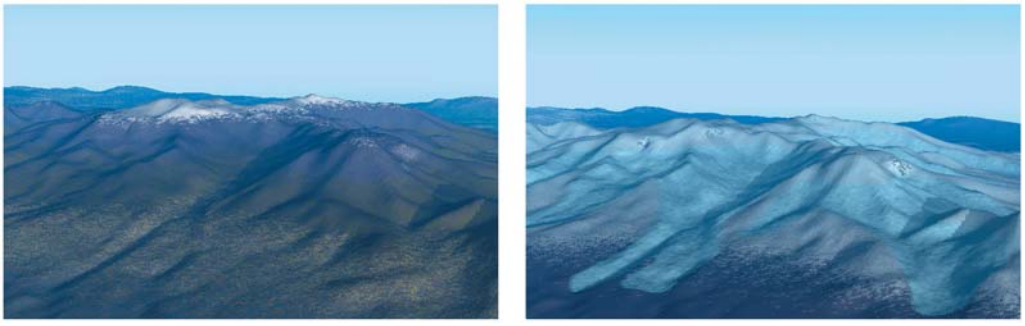
Figure 3: Visualization of actual glaciation (left) and reconstructed Late Quaternary glaciation (right) at Cerro Sillajhuay. Individual glaciers reached down from the strato-volcano into the plain.

4.2 *Central Cordillera de Merida, Andes, Venezuela*

The Rio Chama basin (8º14' to 8º53' N, 70º05' to 71º35' W) is located in the Central Cordillera de Merida of the Venezuelan Andes and peaks in the Pico Bolivar (5007 m asl.) (Fig. 2). In this tropical study area annual precipitation is between 754 mm in the "driest" part of the basin and ~2000 mm in higher altitudes. The field campaign was conducted in summer 2003.

The ASTER level 1B scene dates from March 2003 and is 15% cloud-covered. The study's goal was to assess the role of GCPs from extensive field measurements in DEM quality improvment. Thus, two DEMs were generated and compared: one without using any precise field GCPs (DEM-

A), a second one that included such GCPs from field work (DEM-B). For generation of DEM-A (without field GCPs) stereo-matching included 15 TPs and 50 GCPs taken from imagery orthorectified with SRTM 3-arc-second data merged with 30-arc-second GTOPO30/SRTM data merged at the Jet Propulsion Lab (JPL) and archived at the USGS EROS Data Center. DEM-B (with field GCPs) was generated using the same 15 TPs and in addition ~200 GCPs from field GPS measurements. For the TPs the $RMSE_{x,y}$ was ~18 m, and for the GCPs it was ~7.5 m for channel 3N, and ~18 m for channel 3B. For both cases (DEM-A and DEM-B) the 30-m DEM was generated using: (1) the "low-Z" (low vertical) resolution option, (2) the "high-Z" resolution option of the PCI Geomatica software.

In the case of the "low-Z" resolution DEMs, both DEM-A and DEM-B show similar quality with only few artifacts in cloud-covered areas and some high peaks (Fig. 4). Both DEMs offer information on elevation in 90-95% of the cloud-free areas. In contrast, the results for the "high-Z" resolution option vary between DEM-A and DEM-B. Whereas DEM-B (with field GCPs) still offers elevation information in 80-85% of the cloud-free areas, for the DEM-A (without field GCPs) the elevation information is available for only 60-65% of the cloud-covered areas. The final DEM was generated using the "high-Z" DEM-B (with field GCPs) and fitting the "holes" in a first step with data from the "low-Z" DEM-B (with field GCPs).

All remaining "holes" were filled with data from the GTOPO30/SRTM DEM from JLP. Since at artifact boundaries significant variation in elevation from different DEM data sets occurs, a 7x7 focal mean filter which ignores central value of 7x7 matrix in calculations was used to get seamless transitions.

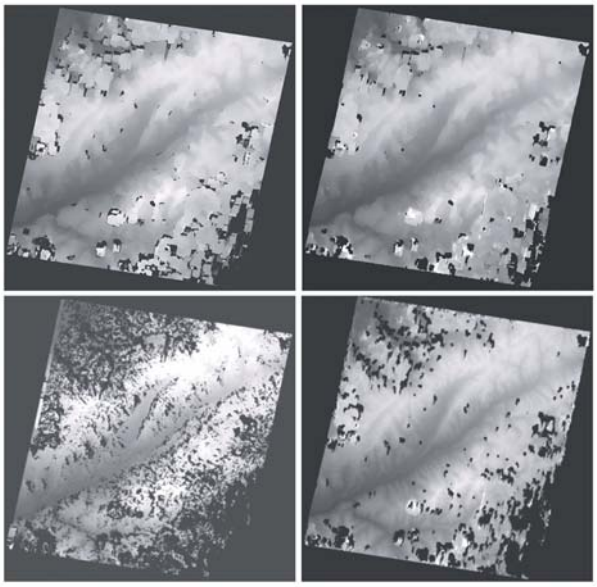

Figure 4: ASTER DEMs for the Cordillera de Merida. Upper left: "Low-Z" resolution option without field GCPs. Upper right: "Low-Z" resolution option with field GCPs. Lower left: "High-Z" resolution option without field GCPs. Lower right: "High-Z" resolution with field GCPs. The results show an increase in DEM quality when using field GCPs.

4.3 *Tirich Mir, Eastern Hindu Kush, Pakistan*

Tirich Mir (7706 m asl., ~36˚ N, ~72˚ W) is located in northern Pakistan (Fig. 2). The pluton is the highest peak of the Hindu Kush and rises ~4000 m above the surrounding valleys. Precipitation mainly occurs in late winter and early spring; it is ~450 mm in 1500 m asl., and up to 2000 mm above 5000 m asl. Field work was undertaken in the summers of 1996-1998.

The ASTER Level 1A scene from September 2002 is nearly cloud-free. Between the stereo-pair 12 TPs and 130 GCPs satellite orthoimagery were collected. The total $RMSE_{x,y}$ was ~6 m for channel 3N, and ~40.5 m for channel 3B. The goal of this study was to identify parameters that affect the DEM accuracy. Results showed that the error increases by 20%, when: (1) slope is >35°; (2) the aspect is between 125° and 350°; (3) the "land cover" is clouds or cloud shadow, but not snow of high reflectance (Fig. 5).

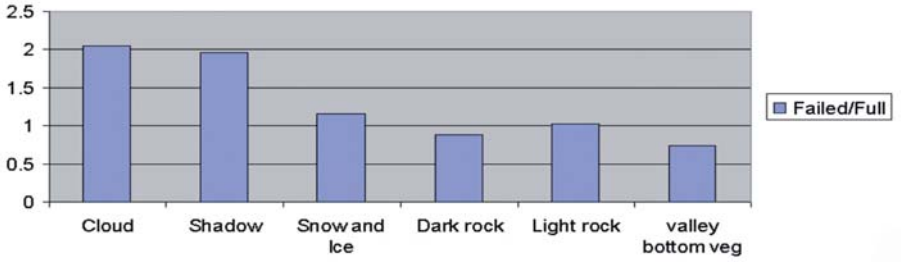

Figure 5: Influence of "land cover" (failed/full ratio) in ASTER DEM generation for the Tirich Mir region, Pakistan. In particular clouds and their shadows result in DEM failure.

4.4 *Northern Tien Shan, Kasakhstan/Kyrgyzstan*

Zailiskiy Alatau and Kungey Alatau (42°30' to 43°30' N, 75° to 79° E) represent the northern part of the Tien Shan at the border between Kasakhstan and Kyrgyzstan (fig. 2). From the Kazkh Steppe at an altitude of about 800 m asl. the two mountain ranges rise up to nearly 5000 m asl. The southern edge is Lake Issyk-Kul (1608 m asl.). The overall continental climate is characterized by sharp local differences. Precipitation varies horizontally between <600 mm in the transition zone to the Kazakh Steppe and ~200 mm at Lake Issyk-Kul, and it reaches >1000 mm in altitudes of >3500 m asl. Fieldwork was undertaken in late summer 2002 and 2003. It included GPS measurements for GCP identification and geomorphological mapping focussing on glacial and periglacial forms. Since fieldwork was restricted to the central part of the northern Tien Shan, geomorphological mapping of the entire area is only possible using satellite data analysis.

Two ASTER Level 1A scenes were selected for analysis: a scene from October 2000 (cloud cover 5%) covers the northern part of the study area; a scene from September 2001 (cloud cover 20%) covers the southern part. In sum, 33 GCPs were collected from fieldwork and topographic maps (1:100 000). Stereo-pair image matching was achieved using 45 tie points (TPs) from different altitudes. The total $RMSE_{x,y}$ was <20 m. The DEM was generated at 30-m resolution with the highest possible level of detail. The quality of the raw DEM was good, since only few artifacts occurred. Nevertheless, cloud-covered areas were marked, clipped and filled with SRTM data of 90-m resolution. SRTM data was also used to fill the gap between the scenes and to extend the DEM in areas not covered by the ASTER scenes. A seamless transition between the two data sets was achieved using a blending procedure offered by the software SAGA.

For evaluation of the DEMs from satellite data, a reference DEM was derived from contour lines from topographic maps 1:100 000 with an equidistance of 40 m. Contour lines from selected valleys were digitized, and the 30-m DEM was generated using a spline interpolation method. Re-

sults show that elevations and contour lines derived from the SRTM DEM match this "reference" DEM nearly perfectly; the average difference is only ~6 m. For the ASTER DEM, the comparison with the SRTM DEM shows some differences in elevation: in the northern Tien Shan elevations are up to 100 m lower at SE-exposed slopes of >35° and up to 50 m higher at N- and NW-exposed slopes (Fig. 5). However, elevations of valley bottoms and mountain ridges are nearly equal in both DEMs, and the average elevation in both DEMs differs only by three meters.

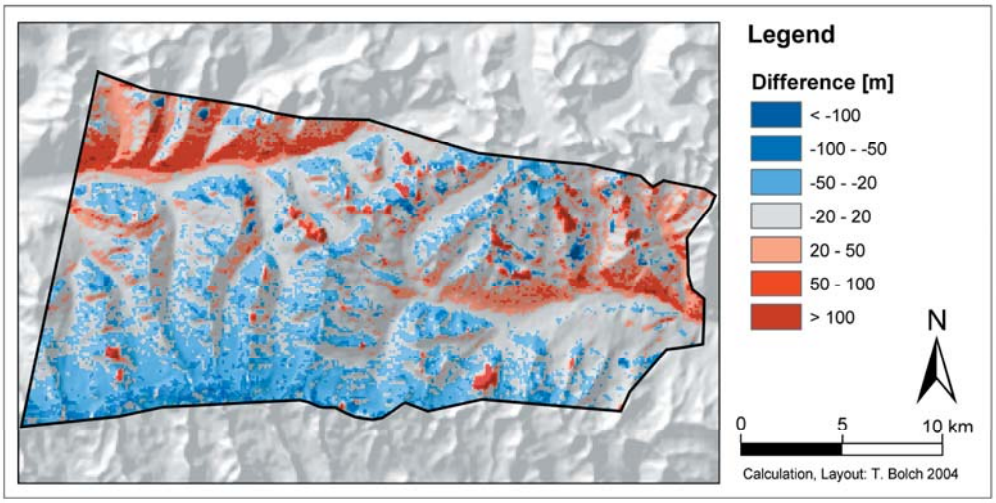

Figure 4: Difference in elevation between SRTM and ASTER DEM for parts of the Tien Shan.

Table 1: Extent of glaciers and rockglaciers in Almatinka valleys and Talgar valley.

	Malaya Almatinka	Bolshaya Almatinka	Lev Talgar
Glaciers			
Total Area [km²]	6,1	17,7	43,6
Portion of Study Area [%]	27,3	18,5	36,9
Elevation [m asl.]	3443 – 4329 Avg.: 3811	3390 – 4570 Avg.: 3870	3440 – 4575 Avg.: 3984
Slope [°]	0,3 – 64 Avg.: 24,3	0,1 – 79 Avg.: 27,5	0,1 – 79 Avg.: 22,4
Rockglaciers			
Total Area [km²]	0,4	7,5	4,2
Portion of Study Area [%]	1,7	7,9	5,0
Elevation [m asl.]	3439 – 3654 Avg.: 3521	3000 – 3900 Avg.: 3425	2730 – 3882 Avg.: 3286
Slope [°]	4,4 – 27,8 Avg.: 11,7	0,2 – 53,3 16,5	0,9 – 44,5 15,6

A detailed geomorphological field mapping focussing on periglacial and glacial forms was carried out in selected valleys in the Zailiskiy Altau. A map of glaciers and rockglaciers was derived using data from topographic maps, field work, satellite images and DEMs.

Using a GIS the areas covered by glaciers and rockglaciers and their elevation and slope were calculated for 1999/2000 (Tab. 1). A comparison with calculations after Vilesov & Uvarov (2001) shows a slightly decrease in extent since 1990.

5 CONCLUSION

ASTER satellite data allow the generation of DEMs of good accuracy for difficult terrain such as high mountain areas. Accuracy increases with the availability of TPs and GCPs covering the entire scene and deriving from different altitudes. Steep slopes, southern slopes of W-E oriented ranges, and clouds/cloud shadows might result in errors ASTER DEM generation, although many artifacts and "critical areas" can be filled with SRTM or merged GTOPO30/SRTM data. In remote high mountains, where the availability of topgraphic maps of high quality is limited, satellite data in general and DEMs ASTER and SRTM in particular are often the only source for studying meso-scale landforms like glaciers, rockglaciers, or moraines. Debis-covered glaciers could be identified using the curvature and slope information from the DEM combined with spectral information from remote sensing data, such as Landsat or ASTER. The DEMs also help in simulations of former landscapes such as Quaternary glaciated terrain. Whereas SRTM DEMs offer more precise elevations, ASTER DEMs offer more details.

ACKNOWLEDGEMENTS

The authors like to thank Manfred Buchroithner (Technical University Dresden) for many helpful discussions and Jens Etter (Humboldt University Berlin) for support in the visualization process of Cerro Sillajhuay. Logistical support and help during field campaigns was provided by Hilmar Schröder (Humboldt University Berlin) in Chile, Jose Roa (University of the Andes – Trujillo) in Venezuela, Klaus Haserodt (Technical University Berlin, †) in Pakistan, Sergej Marchenko (Kazakh Laboratoy of Permafrost) and Volodia Uvarov (Kazakh State University) in Kasakhstan, and Valentina Sankova (Kyrgyz Academy of Sciences) in Kyrgyzstan. Financial support for the four projects was provided by Busch Zantner Foundation (University Erlangen-Nuremberg), DAAD (German Academic Exchange Service), DePaul University (Chicago), DFG (German Research Foundation), and Max Kade Foundation (New York).

REFERENCES

Bishop, M.P., et al. (2001): Topographic analysis and modeling for alpine glacier mapping. *Polar Geography*, 25: 182-201.

Bolch, T. & Kamp, U. (2003): Quality analyses of digital ASTER elevation models of high mountain areas (Cerro Sillajhuay, Chile/Bilovia). Kartographische Nachrichten, 5: 224 - 230. (In German).

Bolch, T. & Schröder, H. (2001): Geomorphologic Mapping and Diversity Analysis of Periglacial Forms at Cerro Sillajhuay (Chile/Bolivia). (Erlanger Geographische Arbeiten, 28), Erlangen, 141 pp. (In German).

Dikau, R., et al. (1995): Morphometric landform analysis of New Mexico. Zeitschrift für Geomorphologie, N.F., Suppl.-Bd., 101: 109-126.

Duncan, C.C., et al. (1998): Comparison of Late Pleistocene and modern glacier extents in central Nepal based on digital elevation data and satellite imagery. *Quaternary Research*, 49: 241-254.

Eckert, S. & Kellenberger, T. (2002): Quality analysis of automatic generated DEMs from ASTER-Data. Publikationen der Deutschen Gesellschaft für Photogrammetrie und Fernerkundung, 11, 337-345. (In German).

Etzelmüller, B. & Sollid, J.L. (1997): Glacier geomorphometry - an approach for analyzing long-term glacier surface changes using grid-based digital elevation models. *Annals of Glaciology*, 24: 135-141.

Hahn, M. (2003): Validation of Digital Elevation Models based on SRTM and ASTER Data. Unpublished M.S. thesis, TU Dresden, pp. 82. (In German).

Kääb, A., et al. (2003): Glacier monitoring from ASTER imagery: accuracy and applications. *EARSeL Proceedings, LIS-SIG Workshop, Berne, March 11-13, 2002*. 43-53.

Kamp, U., Bolch, T. & Olsenholler, J. (2003): DEM generation from ASTER satellite data for geomorphometric analysis of Cerro Sillajhuay, Chile/Bolivia. *Proceedings Annual Meeting Imaging and Geospatial Information Society (ASPRS), 5.-9.5.2003, Anchorage, U.S.A*., 9 pp. (CD).

Kamp, U., Bolch, T. & Olsenholler, J. (2004): Geomorphometry of Cerro Sillajhuay, Chile/Bolivia: Comparison of DEMs from ASTER remote sensing data and Contour Maps. Geocarto International. (In Press).

Paul, F., Huggel, C. and A. Kääb (2004): Combining satellite multispectral image data and a digital elevation model for mapping debris-covered glaciers. Remote Sensing of Environment. 89(4). 510-518.

Paul, F., et al. (2002): *The new remote sensing derived Swiss glacier inventory. I: Methods. Annals of Glaciology*, 34, 355– 361.

Sidjak, R.W. & Wheate, R.D. (1999): Glacier mapping of the Illecillewaet icefield, British Columbia, Canada, using Landsat TM and digital elevation data. *International Journal of Remote Sensing*, 20: 273-284.

Vilesov, E.N. & Uvarov, V. N. (2001): *The Evolution of Modern Glaciation of the Sailiskiy Alatau in the 20th Century*. Kazakh State University, Almaty, pp. 252. (In Russian).